

ChemComm

Accepted Manuscript



This is an *Accepted Manuscript*, which has been through the Royal Society of Chemistry peer review process and has been accepted for publication.

Accepted Manuscripts are published online shortly after acceptance, before technical editing, formatting and proof reading. Using this free service, authors can make their results available to the community, in citable form, before we publish the edited article. We will replace this *Accepted Manuscript* with the edited and formatted *Advance Article* as soon as it is available.

You can find more information about *Accepted Manuscripts* in the [Information for Authors](#).

Please note that technical editing may introduce minor changes to the text and/or graphics, which may alter content. The journal's standard [Terms & Conditions](#) and the [Ethical guidelines](#) still apply. In no event shall the Royal Society of Chemistry be held responsible for any errors or omissions in this *Accepted Manuscript* or any consequences arising from the use of any information it contains.



ChemComm

COMMUNICATION

Reversibly photoresponsive switching in Bi_{2.5}Na_{0.5}Nb₂O₉-based luminescent ferroelectrics

Received 00th January 20xx,
Accepted 00th January 20xx

Qiwei Zhang,^{a*} Haiqin Sun,^a Hao Li,^a Xusheng Wang,^b Xihong Hao,^{a*} Jinling Song^a and Shengli An^a

DOI: 10.1039/x0xx00000x

www.rsc.org/chemcomm

Reversible luminescence modulation upon photochromic reactions with excellent reproducibility was achieved from Eu³⁺ doped Bi_{2.5}Na_{0.5}Nb₂O₉ multifunctional ferroelectrics. The material exhibits strong sensitivity to visible light or sunlight with fast response time without inducing any structure changes.

Luminescent photochromic (PC) materials are gradually considered to be one of the most important active materials, and have been extensively studied owing to their potential applications in photonic devices, such as photo-switching, optical memory systems and sensors etc.¹ In particular, photo-responsive modulation of luminescence emission intensity is regarded as a promising strategy to realize non-destructive readouts and security recordings of PC materials, and achieve ultra-high data storage densities and fast data-processing rates. A alternative approach to modulate luminescence is to combine some photochromic compounds with some luminescent moieties, such as organic π -conjugated molecules, metal complexes and nanocrystals.²⁻⁴ However, in most organic molecules such as fluguides, diarylethenes, terarylenes or their derivatives, it is difficult to obtain this ideal candidate molecule possessing the ability to turn luminescence “on” or “off”, without inducing some structure reactions.⁵⁻⁷ So far, considerable attention has been focused on the luminescence switching properties of organic compounds, whereas only a few studies have been carried out concerning the photochromic luminescence control of inorganic materials, especially their related mechanism of luminescence modulation still unclear, owing to the notable difference of molecule structures between inorganic and organic compounds.

Despite very few studies on luminescence modulation of inorganic materials, they remain fairly attractive owing to their excellent thermal stability, mechanical strength and chemical resistance, which can be expected as compact high density optical

memory materials with very small laser diodes, as compared to organic PC materials.⁸⁻¹⁰ Although some inorganic materials display PC performance, such as: Sr₂SnO₄:Eu³⁺,¹¹ BaMgSiO₄:Eu³⁺ etc.,¹² no luminescence modulation behavior based on photochromic reaction is observed.

Here, we report a novel inorganic PC material very sensitive to visible light (465 nm) or sunlight: Eu³⁺ doped Na_{0.5}Bi_{2.5}Nb₂O₉, which shows a reversible luminescence modulation performance with excellent reproducibility. Meanwhile, we demonstrate in detail the mechanism of luminescence-switching phenomenon by in-situ measuring spectral changes upon photochromic reactions.

Eu³⁺ doped Na_{0.5}Bi_{2.5}Nb₂O₉ materials were designed according to the formula: (Na_{0.5}Bi_{0.5})_{1-x}Eu_xBi₂Nb₂O₉ (x=0.10, 0.20, 0.30, 0.4), abbreviated as NBN:xEu, and fabricated by solid-state sintering method. The Na₂CO₃ (Alfa Aesar, 99.5%), Bi₂O₃ (Alfa Aesar, 99.975%), Nb₂O₅ (Alfa Aesar, 99.5%), Eu₂O₃ (Alfa Aesar, 99.9%) powders as starting materials were weighted. Sample preparation, structure, composition and luminescence property characterization were described in the supporting information (see ESI, S1).

Fig. 1a gives XRD patterns of all samples. From which, the diffraction peak positions can be indexed based on the standard diffraction data of NBN (PDF#42-0397) with the *A*₂₁*am* space group. No additional peaks were found except for a little amount of secondary phase of BiNbO₄, which means that Eu³⁺ ions have diffused into NBN matrix to form solid solutions as desired. The plate-like SEM image with x=0.10 is obvious observed, as shown in Fig. 1b, showing the typical Aurivillius type structure caused by the anisotropic nature of the crystal structure, depicted in Fig. 1c.¹³ We adopted the ICP-AES to investigate the loss and deviation degree from the stoichiometric ratio due to volatility of alkali elements, as shown in Fig. 1d. In comparison with theoretical stoichiometric ratio, the volatilization of Na is more serious than Bi. According to these results, the volatilization of Na or Bi would produce a certain amount of defects and vacancies, which may play an important role in PC behavior and luminescence modulation performance.

^a School of Materials and Metallurgy, Inner Mongolia University of Science and Technology, 7# Arerding Street, Kun District, Baotou 014010, China. E-mail: zqw8000@imust.edu.cn; xhhao@imust.edu.cn

^b Functional Materials Research Laboratory, School of Materials Science and Engineering Tongji University, 4800 Caoyang Road, Shanghai 201804, China

†Electronic Supplementary Information (ESI) available: Experimental procedures O1s and Bi 4f fitting parameters, Reflectance intensity changes and Fitting equation. See DOI: 10.1039/x0xx00000x

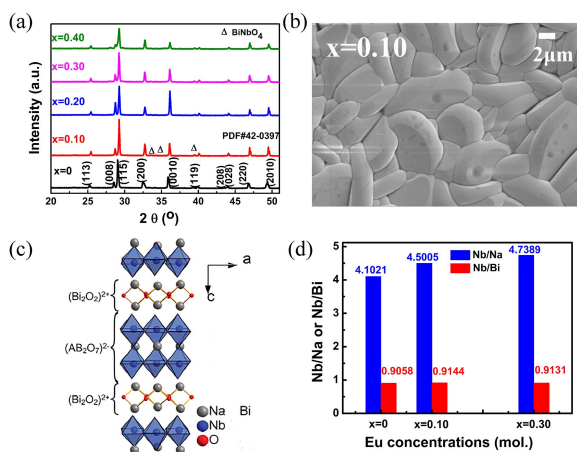


Fig. 1 (a) XRD patterns of NBN: x Eu samples. (b) SEM image of the representative composition $x=0.10$. (c) Crystal structure viewed along [010] direction.¹³ (d) Nb/Na and Nb/Bi mole ratio of NBN: x Eu ($x=0, 0.10, 0.30$).

Fig. 2 shows the photochromic reaction process and reflection spectra changes upon the simulated sunlight irradiation and thermal stimulus in Eu doped NBN samples. In Fig. 2a, the NBN: x Eu samples undergo a thermally reversible photochromism from a colored state to a dark colored state upon sunlight or visible light irradiation. Before light irradiation, samples exhibit a change from green color to pale yellow with increasing Eu concentrations, whereas the color of samples quickly turns dark grey with sunlight irradiation. When the dark grey sample is heated up to 200 °C for 10 min, it will once recover their initial color. And, the coloration and de-coloration process is reversible and can be repeatedly switched. Fig. 2b gives the changes in reflection spectra for the representative sample of NBN: 0.30Eu after exposure to sunlight for 0s and 5s, respectively. A broad absorption occurs at visible light region from 400 nm to 700 nm, the strongest absorption, is located at approximately 460 nm, determined by $Abs=R(0)-R(5s)$, ($R(0)$ and $R(5s)$: the reflectance intensity of 0s and 5s irradiation). The reflectance spectra only exhibits very weak changes even after 10s, 20s irradiation or more time, similar behavior is observed in other compositions (Fig. S1, ESI). Fig. 2(c) shows that the NBN:0.30Eu sample has good reversibility during the coloration-decoloration process. The reversibility can be improved by Eu doping, as shown in Fig. S2 (ESI), especially for $x=0.30$ composition. The strongest absorption values have a slight change with increasing Eu concentrations, as shown in Fig. 2d, the optimized absorption value is about 24.5 for $x=0.10$.

The PL and PLE spectra of the NBN: 0.30Eu are shown in Fig. 3 at room temperature. The excitation spectrum, monitored at 618 nm, consists of two strong narrow absorptions, wherein the band at 395 nm coming from the ${}^7F_0 \rightarrow {}^5L_6$ transition, the 465 nm band coming from the ${}^7F_0 \rightarrow {}^5D_2$ transition. The strongest sharp peak appears in the blue light region (465 nm). The emission spectrum excited at 465 nm exhibits a strong line emission peak centered at 618 nm and a weak line emission peak at 595 nm. These two strong emission peaks are attributed to the ${}^5D_0 \rightarrow {}^7F_1$ (595 nm) and ${}^5D_0 \rightarrow {}^7F_2$ (618 nm) transitions, respectively. The excitation spectrum strongly overlaps with the near ultraviolet-visible light range of the solar spectrum,¹⁴ suggesting that the NBN: x Eu sample excited at 465 nm not only

possesses PC performance, but also exhibits the strong red emission at 618 nm.

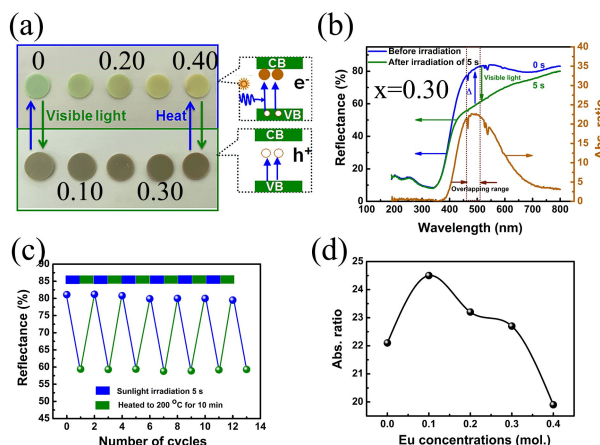


Fig. 2 (a) Photographs of NBN: x Eu before and after sunlight irradiation. (b) Reflection spectra for the NBN:0.30Eu by visible light irradiation (0s, 5s, 10s) and the difference absorption (Abs). (c) Reflectance intensity changes of the NBN: 0.30Eu upon alternating sunlight irradiation (AM 1.5) and heating treatment. (d) The strongest absorption (Abs.) vs. Eu concentrations.

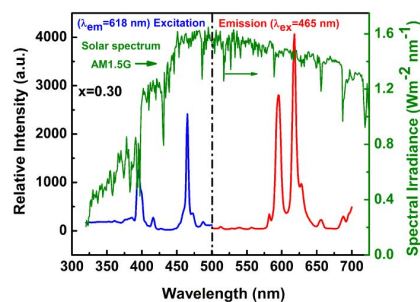


Fig. 3. Excitation ($\lambda_{em}=618$ nm) and emission ($\lambda_{ex}=465$ nm) spectra of the NBN:0.30Eu material at room temperature. The green solid line is the solar spectrum received at the Earth's surface at the air mass 1.5 global (AM 1.5) condition.¹⁴

Due to the absorption bands well agreed with the excitation wavelength, the excitation light simultaneously acts as irradiation light source, thus this feature can realize *in-situ* PL measurement without interrupting irradiation, schematically illustrated in Fig. 4a. The PL spectral changes of $x=0.30$ sample upon irradiation with near UV light ($\lambda_{ex}=395$ nm) and visible light ($\lambda_{ex}=465$ nm) are shown in Fig. 4b and 4c. The emission intensity at 595 nm and 618 nm is obviously quenched with the increase of irradiation cycle. Meanwhile, the irradiated area shown in Fig. S3 gradually turns dark grey color (ESI). In comparison, the PL change is much significant upon 465 nm irradiation than that upon 395 nm irradiation, as determined from the relative intensity ratio of the ${}^5D_0 \rightarrow {}^7F_2$ (618 nm) transitions at every cycle against its initial emission intensity. The ratio is obtained by the formula: $\Delta R_n = (R_0 - R_n) / R_0 \times 100\%$, where R_0 and R_n are the initial intensity and the relative intensity under different irradiation cycles (n), respectively. The ΔR_n value as a function of irradiation cycles is illustrated in Fig. 6d. The PL intensity almost decreases to 52.77% of its initial intensity under 465 nm irradiation of 20 cycles, whereas only 38.2% under 395 nm

irradiation. The difference in the relative intensity ratio under different excited wavelength indicates that the luminescence modulation upon photochromic reaction is sensitive to visible light region ($\lambda > 400$ nm). Similar results are observed in PLE spectral changes of x=0.30 sample monitored at 618 nm ($\lambda_{em}=618$ nm) under different irradiation cycles, as shown in Fig. S4 (ESI).

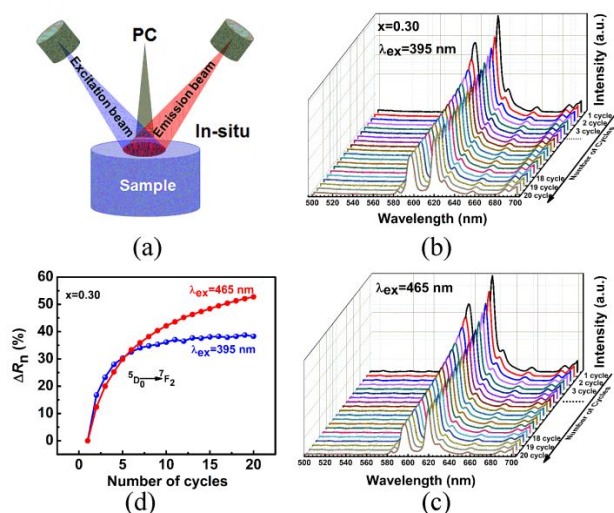


Fig. 4 (a) Schematic of *in-situ* luminescence modulating upon PC reactions. (b) and (c) PL spectral changes of the NBN:0.30Eu sample excited at 395 nm and 465 nm under different irradiation cycles at room temperature, respectively. (d) The luminescence quenching degree (ΔR_n) as a function of irradiation cycles at $\lambda_{ex}=395$ nm and $\lambda_{ex}=465$ nm.

Similar luminescence quenching behavior is also observed in other compositions, as shown in Fig. 5. From which, it is obviously observed that the ΔR_n value gradually increases with Eu concentrations, and reaches a maximum as Eu doping content is up to 0.30 mol under 465 nm or 395 nm irradiation of 20 cycle. In comparison, the ΔR_n value excited at 465 nm irradiation is obviously higher than that at 395 nm. But, the maximal ΔR_n value occurs at $x=0.30$, which contradicts to the results of Fig. 2d. Apart from the factor of the absorption ratio, electron energy level transitions from Eu ions should be also considered, the competition between these two factors results in the strongest luminescence quenching occurring at $x=0.30$ mol (Fig. 2d and the inset of Fig. 5).

Likewise, the reproducibility for the luminescence modulation upon photochromic reactions is also a very important parameter to evaluate the cycle stability of non-destructive readout. Fig. 6 shows the reversible luminescence modulation of NBN: xEu ($x=0.10, 0.20, 0.30$, and 0.40) samples upon 465 nm irradiation after 5 periods between two coloration states, wherein every period includes 20 cycles. After *in-situ* irradiated 20 cycles at room temperature, its PL intensity from the $^5D_0 \rightarrow ^7F_2$ can well recover its initial state as the sample is heated to 200 °C for 10 min. Most importantly, the luminescence could be repeatedly switched upon PC reactions by *in-situ* PL measurements, and the PL intensity has no significant degradation after several periods, showing excellent reproducibility.

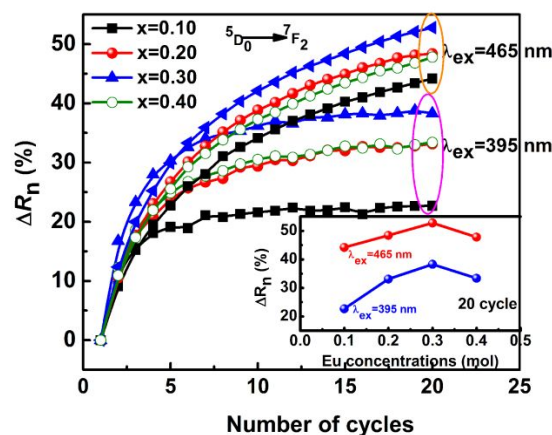


Fig. 5 The ΔR_n dependence on different irradiation cycles for NBN: xEu, the inset is the ΔR_n as a function of Eu concentrations excited at 395 nm and 465 nm.

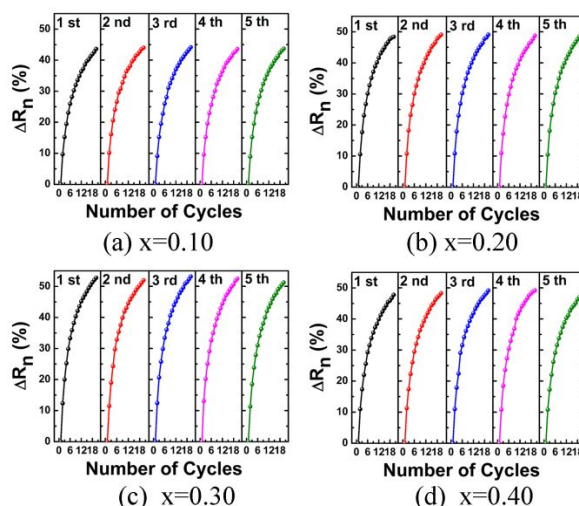


Fig. 6 Reproducibility of the luminescence modulation of NBN: xEu upon alternating 465 nm visible light and heat treatment under 5 periods.

Based on our experimental results and the trapped charge carrier model, we propose the following luminescence modulation mechanism upon PC reactions for Eu^{3+} doped NBN.

Photochromism-decoloration: When the sample is irradiated with visible light ($\lambda > 400$ nm), an electron transition from O-2p orbitals to Bi and Eu-4f orbitals occurs.¹² These photo-generated electrons in conduction band are usually trapped by oxygen vacancies or captured by the reduction of Bi^{3+} to a sub-oxidized bismuth state with Bi^{3-x} ($x > 0$), then forming color centers in NBN: xEu, similar to $\text{BaMgSiO}_4:\text{Eu}^{2+}$ and $\text{Sr}_2\text{SnO}_4:\text{Eu}^{3+}$,^{12,13} giving rise to strong absorption in the visible light region. The transfer process above could lead to the reaction of Nb and A site ions adjacent to oxygen bonds: Nb-O and A(Bi, Na)-O bonds.^{15,16} In order to prove the process, the fitted O 1s and Bi 4f XPS spectra before and after visible light irradiation of 5s were investigated, as shown in Fig. S5a, b (ESI) and Fig. 7. The fitting parameters are listed in Table S1 (ESI). From the spectra changes of O 1s before and after irradiation,

shown in Fig. S4 (ESI), we clearly observe that the peaks shift to higher energy side, not found in other elements (such as, Na 1s, Eu 3d, Bi 4f and Nb 3d). A possible interpretation of this observed positional shift is that there is a weak electrostatic interaction, showing lower electronegativity of oxygen ions from A-O and Nb-O bonds, the origin is obviously coming from the electrons trapped by oxygen vacancies and Bi ions, the process is also confirmed by the decrease of the ratio between lattice oxygen and absorbed oxygen (V_o/O^{2-}) after irradiation, as shown in Table S1 (ESI).¹⁵ Meanwhile, Bi 4f spectra of NBN: xEu are shown in Fig. 7 under non-irradiation and 5 s irradiation time. One "shoulder" peak appears at lower energy sides of the Bi 4f_{7/2} and Bi 4f_{5/2} peaks, located at 158.53 eV and 163.83 eV, respectively. After irradiation, those "shoulder" peaks become more intensive, which may come from a suboxidated bismuth with Bi^{3-x}, while the major Bi 4f doublet peaks have no obvious changes (assigned to the oxidized bismuth Bi³⁺).¹⁵ The increase of relative intensity of the sub-oxidated bismuth (Bi^{3-x}) after irradiation indicates more and more electron captured by Bi³⁺. These results also prove our statements of photochromism mechanism discussed above in NBN: xEu.

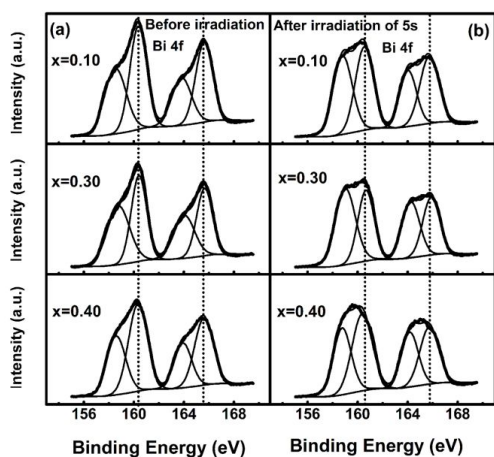


Fig. 7 (a) Before irradiation and (b) After irradiation of sunlight Bi 4f XPS spectra for NBN: xEu ($x=0.10, 0.30, 0.40$) samples.

Luminescence modulation upon photochromic reactions: As suggested in Fig. 4 and 5, the luminescence emission intensity or ΔR_n changes are directly linked to the irradiation cycles caused by photochromic reaction. During the *in-situ* PL measurements, the PC process and PL emission simultaneously happen (Fig. 4 and Fig. S3), which indicates that the photo-generated electrons can be divided in two parts, wherein one part is coming from NBN matrix, the other part is coming from the Eu ions. The electrons from NBN matrix are responsible for PC, no luminescence at 618 nm is observed. The electrons from Eu low energy levels (7F_0) can be excited to a higher level of 5L_6 and 5D_2 , and recombine to lower levels, then leading to red emission. The emission intensity monotonously decreases with increasing irradiation cycles (Fig. 4), indicating that only a portion of the excited state electrons of Eu ions beneficial to red emission. Another portion of the excited state electrons from Eu ions should be captured by vacancy-related defects forming color centers. With gradually increasing irradiation cycles or time, more and more excited electrons are trapped

without being recombined, thus suppressing the PL emission. Therefore, we can conclude that the dynamic luminescence quenching changes should lie on the light absorption behavior, which is supported by the fitting results to the relaxation model, as shown in Fig. S6.¹⁷

CONCLUSIONS

A novel inorganic photochromic material of Eu³⁺ doped NBN was obtained by the conventional solid reaction method. Under visible light (465 nm) or sunlight irradiation, the material exhibited a reversible photochromism between green-yellow and green color by alternating visible light irradiations (465 nm) and thermal stimulus. Meanwhile, the luminescence emission intensity can be effectively modulated and reversibly switched without any deterioration of the switching properties, indicating the luminescence modulation with nondestructive readout capability of this system.

This work was supported by the Natural Science Foundation of China (No. 51562030 and 201407084), the Natural Science Foundation of Inner Mongolia (No. 2015BS0503) and the Research Fund for Higher Education of Inner Mongolia (No. NJZY13141).

Notes and references

- (a) M. Irie, *Chem. Rev.*, 2000, 100, 1685; (b) H. Tian and S. Yang, *Chem. Soc. Rev.*, 2004, 33, 85.
- M. Taguchi, T. Nakagawa, T. Nakashima and T. Kawai, *J. Mater. Chem.*, 2011, 21, 17425; (b) Y. Hasegawa, T. Nakagawa and T. Kawai, *Coord. Chem. Rev.*, 2010, 254, 2643.
- (a) T. Kawai, T. Sasaki and M. Irie, *Chem. Commun.*, 2001, 711; (b) M. Irie, T. Fukaminato, T. Sasaki, N. Tamai and T. Kawai, *Nature*, 2004, 420, 759; (c) T. Fukaminato, T. Sasaki, T. Kawai, N. Tamai and M. Irie, *J. Am. Chem. Soc.*, 2004, 126, 14843.
- M. Heilemann, P. Dedecker, J. Hofkens and M. Sauer, *Laser Photon. Rev.*, 2009, 1-2, 180.
- H. Tian and S. Wang, *Chem. Commun.*, 2007, 781.
- C. J. Yun, J. You, J. Kim, J. Huh and E. Kim, *J. Photochem. Photobiol. C: Photochem. Rev.*, 2009, 10, 111.
- D. Gust, T.A. Moore and A.L. Moore, *Chem. Commun.*, 2006, 1165.
- S. Nishio and M. Kakihana, *Chem. Mater.*, 2002, 14, 3730.
- (a) J.N. Yao, K. Hashimoto and A. Fujishima, *Nature*, 1992, 355, 624; (b) T. Yamase, *Chem. Rev.*, 1998, 98, 307; (c) T. He and J.N. Yao, *J. Mater. Chem.*, 2007, 17, 4547.
- R. Pardo, M. Zayat and D. Levy, *Chem. Soc. Rev.*, 2011, 40, 672.
- S. Kamimura, H. Yamada and C.N. Xu, *Appl. Phys. Lett.* 2013, 103, 031110.
- M. Akiyama, *Appl. Phys. Lett.*, 2010, 97, 181905.
- C. B. Long, H. Q. Fan, M. M. Li and Q. Li, *Cryst. Eng. Comm.* 2011, 14, 7201.
- Z. W. Pan, Y. Y. Lu and F. Liu, *Nat. Mater.*, 2012, 11, 58.
- C. B. Long, H. Q. Fan and P. R. Ren, *Inorg. Chem.* 2013, 52, 5045.
- J. A. Armstrong and M. T. Wellar, *Chem. Commun.* 2006, 1094.
- T. Saitoh, A. E. Bocquet, T. Mizokawa, H. Namatame, A. Fujimori, M. Abbate, Y. Takeda and M. Takano, *Phys. Rev. B* 1995, 51(20), 13942.